Transient Analysis of a New Outer-Rotor Permanent-Magnet Brushless DC Drive Using Circuit-Field-Torque Coupled Time-Stepping Finite-Element Method

Yong Wang, K. T. Chau, *Member, IEEE*, C. C. Chan, *Fellow, IEEE*, and J. Z. Jiang

Abstract—In this paper, a new outer-rotor permanent magnet (PM) brushless dc drive is designed and analyzed. To enable this drive applicable to electric vehicles, its transient performances at both normal and flux-weakening operations are particularly focused. The distinct feature in design is due to the new motor configuration including the outer-rotor topology, the multipole magnetic circuit and the full slot-pitch coil span arrangement. The distinct feature in analysis is due to the development of the circuit-field-torque coupled time-stepping finite-element method. The proposed PM brushless dc drive is prototyped. The analysis results are verified by experimental measurement.

Index Terms—Brushless dc machines, permanent magnet machines, time-stepping finite-element method.

I. INTRODUCTION

WITH EVER increasing concerns of energy conservation and environmental protection, the development of EVs is being accelerated. One of the key EV technologies is the electric drive, which aims to offer high efficiency, high power density, wide speed range and good dynamic performance [1]. Among advanced electric drives, the PM brushless dc drive is most promising [2], [3]. In recent years, the application of the FEM to the steady-state analysis of the PM brushless dc drive has been a success [4].

The purpose of this paper is to design and analyze a new outer-rotor PM brushless dc drive specially for EVs. Because of the aforementioned stringent requirements of the EV drive, both the motor configuration and the analysis approach need to be innovative.

II. OUTER-ROTOR PM BRUSHLESS DC DRIVE

A. Machine Design

The schematic configuration of the proposed PM brushless dc machine is shown in Fig. 1. The machine was designed as
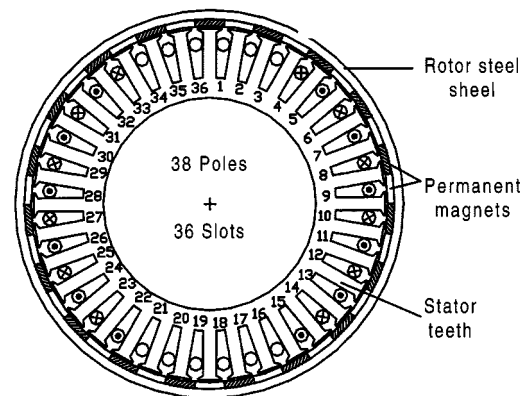
Fig. 1. Proposed PM brushless dc machine.

a low-speed, high-torque outer-rotor type machine, suitable for direct drive of electric bikes and no gear reduction is needed. The machine has 38 poles and 36 slots.

On the inner surface of the proposed machine, 38 pieces of PM are mounted alternately to form 38 poles and two adjacent poles make up a pair of poles so that the flux paths of different pole pairs are independent. This multipole magnetic circuit arrangement enables to reduce the magnetic iron yoke, resulting in the reduction of volume and weight. The coil span of stator windings is designed to be equal to the slot pitch, the overhanging part of the coil can be significantly reduced, thus resulting in the saving of copper as well as the further reduction of volume and weight. By using the fractional number of slots per pole per phase, the magnetic force between the stator and rotor at any rotating position is uniform, thus minimizing the cogging torque that usually occurred in PM brushless dc machines.

B. Principle of Operation

As shown in Fig. 1, the slots 34–3 and 16–21 belong to phase A, the slots 10–15 and 28–33 to phase B, and the slots 22–27 and 4–9 to phase C. The polarity of the shaded PM is S while the nonshade PM is N.

At the position as shown in Fig. 1, phase A is in nonconducting state, while phase B and phase C is conducting. The interaction between the PM excitation field and the current of phase B and phase C generates a clockwise torque on the windings. Since the windings are fixed on the stator, the counterforce will drive the PM rotating anticlockwise.

At any moment, there are two phase windings in conducting state and one-phase winding in nonconducting state. Each phase winding conducts $120°$, and nonconducts $60°$, both in positive and negative directions, whereas the phase shift between adjacent phases is $60°$.

There are two operation mode for the proposed machine, namely the constant torque (normal mode) and the constant power (flux-weakening mode). At the normal mode, the conducting state solely depends on the position signal. At the flux-weakening mode, the phase advance method is applied. The key of this method is to employ the transformer EMF which is proportional to the derivative of phase current to counteract the rotational EMF that is even larger than the applied voltage at high speeds [5]. At this mode, the conducting state depends on the combined signal of position and advanced angle.

III. ANALYSIS APPROACH

The two-dimensional (2-D) circuit-field-torque coupled time stepping finite-element method is employed to analyze the proposed machine. The governing equation for electromagnetic field is given by

$$\nabla \times \upsilon \nabla \times A = J \qquad (1)$$

where υ stands for reluctivity, A for magnetic vector potential which is assumed to have axial component only and J for current density. In the area of iron and air gap, the field equation can be written as

$$\nabla \times \upsilon \nabla \times A = \partial A / \partial t. \qquad (2)$$

At the rotor PM area, the field equation can be expressed as

$$\nabla \times \upsilon \nabla \times A = \upsilon \nabla \times M \qquad (3)$$

where M stands for magnetization of the permanent magnets. In the area of each phase conductor, J can be calculated by

$$J = \sigma(V_b / l + \partial A / \partial t) \qquad (4)$$

where σ stands for electrical conductivity, l for the effective length of conductors connected in series per phase and V_b for conductor voltage drop on the effective length. Thus, in this area, the field equation can be rewritten as

$$\nabla \times \upsilon \nabla \times A = \sigma(V_b / l + \partial A / t). \qquad (5)$$

Since the proposed machine is controlled by a six step inverter, the applied voltage of each phase stator winding is known while the stator current is unknown. The circuit equation of the proposed machine can be expressed as

$$[V_S] = [L][dI/dt] + [R][I] + [V_b] \qquad (6)$$

where $[V_S]$ stands for applied voltages, $[L]$ for end inductance, $[I]$ for phase current and $[R]$ for end resistance. Combining (4) and (6), it yields

$$J = \sigma\{-(1/l)([L][dI/dt] + [R][I]) + [V_S]/l\} + \sigma(\partial A/\partial t). \qquad (7)$$
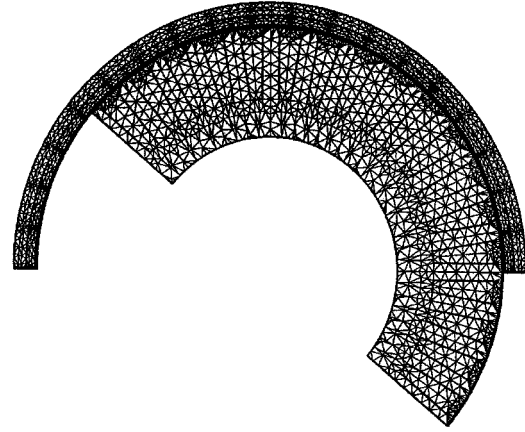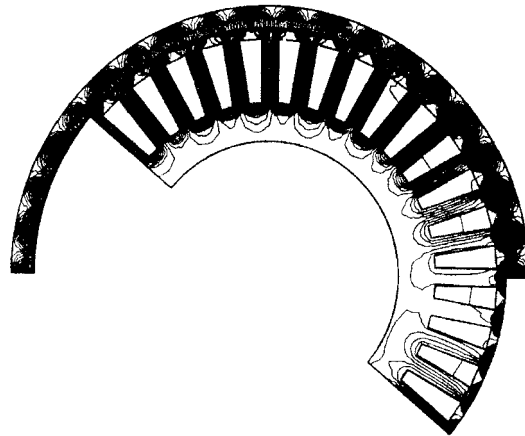

Fig. 2.   FEM mesh.

Fig. 3.   Flux distribution at rated operation.

Hence, the circuit equation can be coupled with the magnetic field equation by the use of (1) and (7).

By using finite-element discretization of the circuit-field equations, we obtain

$$[C]\begin{bmatrix} A \\ I \end{bmatrix} + [D]\begin{bmatrix} \partial A/\partial t \\ \partial I/\partial t \end{bmatrix} = [P] \qquad (8)$$

where $[C]$ and $[D]$ are coefficient matrices, $[A]$ and $[I]$ are unknown and $[P]$ is the vector associated with applied voltage and magnetization of PM. For simplicity, this system equation can be expressed as

$$[C][X] + [D][\partial X/\partial t] = [P]. \qquad (9)$$

The backward Euler difference method is applied for time stepping discretization as follows:

$$([C_k] + [D_k]/\Delta t)[X_k] = [P_k] + ([D_k]/\Delta t)[X_{k-1}] \qquad (10)$$

where the subscript k stands for the kth time step, $\Delta t = t_k - t_{k-1}$ is the kth time step size.

The torque equation of the proposed machine is given by

$$J_m(d\omega/dt) + \lambda\omega = T_e - T_f \qquad (11)$$

where J_m stands for the moment of inertia, ω for rotor speed, λ for coefficient of friction, T_e for the electromagnetic torque
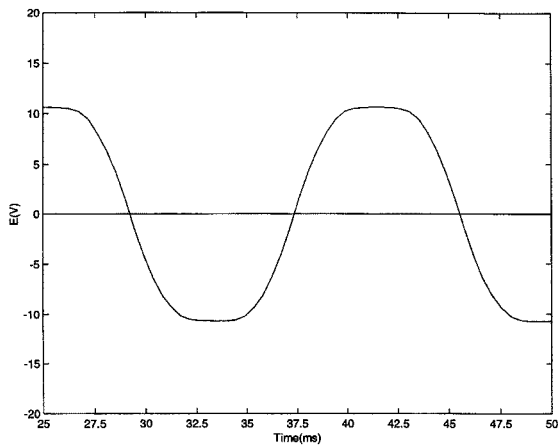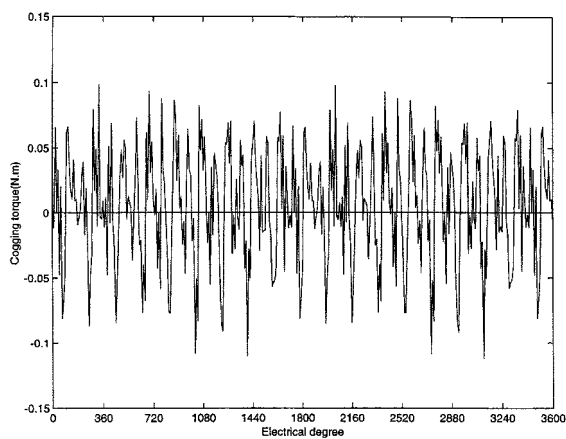
Fig. 4. Calculated back EMF waveform.

Fig. 5. Calculated cogging torque.

Fig. 6. Calculated phase current waveform.

Fig. 7. Calculated speed transient waveform.
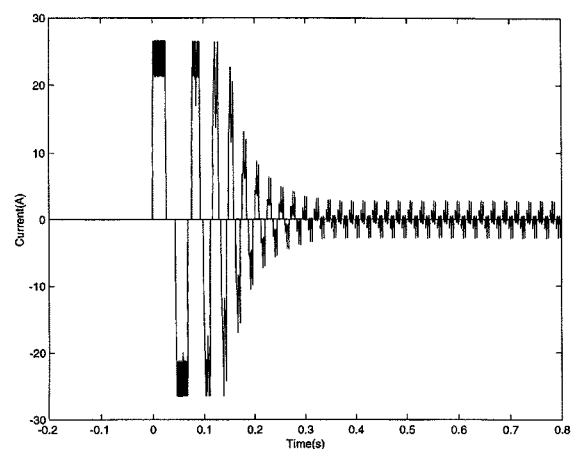
Fig. 8. Calculated phase current transient waveform.

and T_f for load torque. The circuit-field equation is coupled to the torque equation through the electromagnetic torque T_e. At each time step, the electromagnetic torque is calculated using Maxwell stress tensor method. Then, the rotor velocity and the rotor position can be determined. The rotor mesh moves according to rotor movement. During the rotation of the rotor mesh, the slide surface technique is employed to avoid the re-shape of the rotor mesh.

In order to combine flux-weakening control strategy, at each time step the applied voltage will be determined not only by the rotor position but also by the reference of advanced conduction angle. By the use of (10) and (11), the performance of the proposed machine can be determined.

IV. ANALYSIS RESULT

The finite-element mesh of the proposed machine is shown in Fig. 2 and the flux distribution is shown in Fig. 3. Fig. 4 shows the calculated back EMF waveform of the proposed machine when it is running at rated operation. Fig. 5 shows the calculated cogging torque of the proposed machine. Fig. 6 shows the steady state phase current waveform when the machine is running at rated operation Figs. 7–9 show the transient responses of speed, phase current and torque, respectively. Increasingly, Fig. 8 shows that during starting period the current is regulated to maintain its maximum allowable value in such a way that the
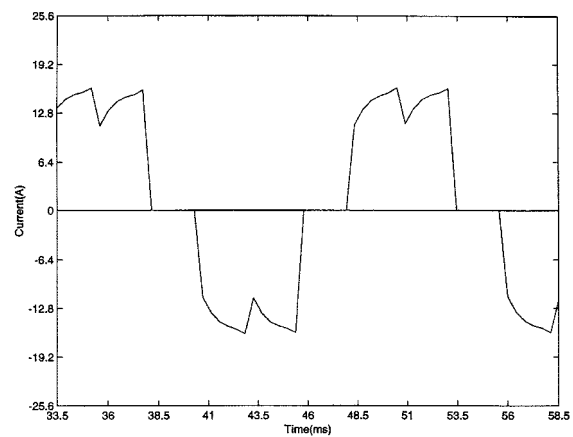
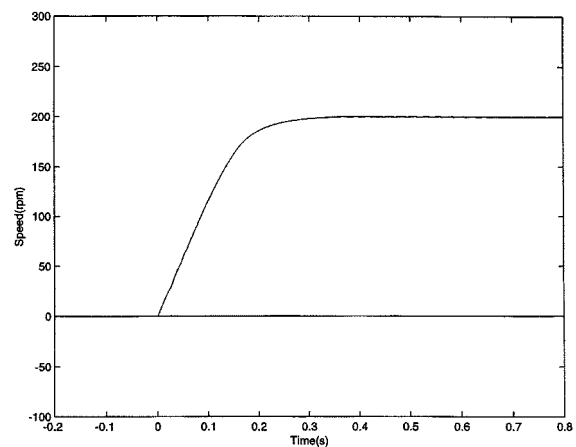maximum allowable starting torque, constant acceleration and fast response can be achieved. Also, Fig. 10 shows the phase current waveform when the proposed machine is running at 2.5 times the base speed with 50° advanced conduction angle.

V. EXPERIMENTAL RESULTS

Figs. 11–13 show the measured back EMF and phase current waveforms and transient speed response, respectively.
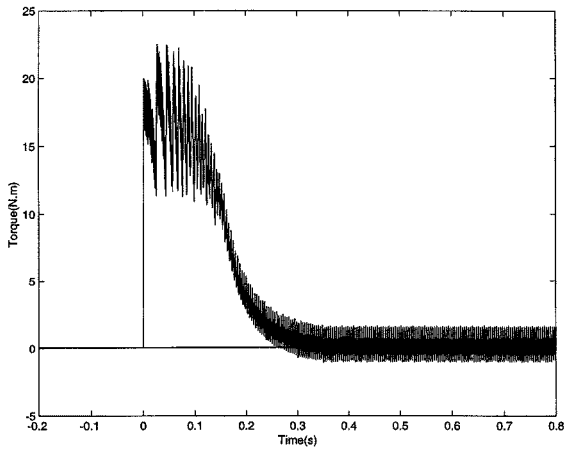
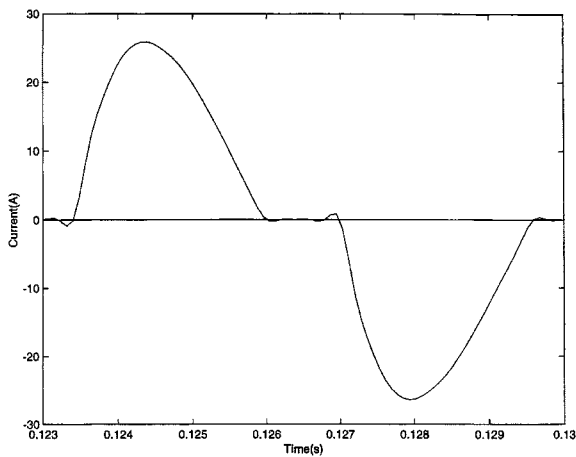Fig. 9. Calculated torque transient waveform.

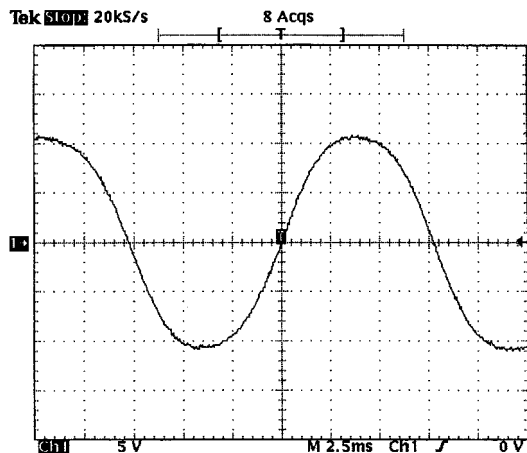Fig. 10. Calculated phase current waveform at flux-weakening mode.

Fig. 11. Measured back EMF waveform (2.5 ms/div, 5 v/div).

Compared with the analysis results, it can be seen that the theoretical and experimental results agree closely.
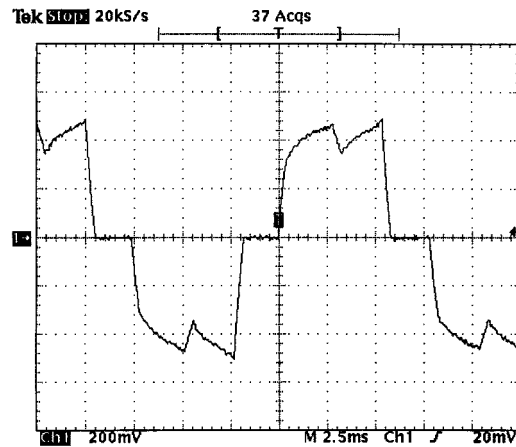

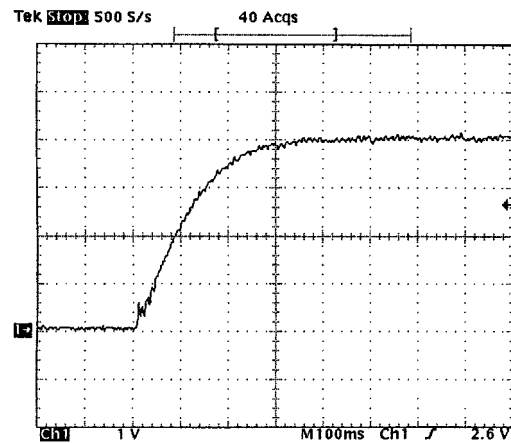Fig. 12. Measured phase current waveform (2.5 ms/div, 6.4 A/div).

Fig. 13. Measured speed transient waveform (100 ms/div, 50 rpm/div).

VI. CONCLUSION

A new outer-rotor PM brushless dc machine has been designed for EV application. The proposed machine is analyzed with the circuit-field-torque coupled time-stepping FEM. Analysis results of the steady state and transient state performance are presented and well supported by experimentation.

REFERENCES

[1] C. C. Chan and K. T. Chau, "An overview of power electronics in electric vehicles," *IEEE Trans. Ind. Electron.*, vol. 44, pp. 3–13, Feb. 1997.
[2] C. C. Chan, K. T. Chau, J. Z. Jiang, W. Xia, M. Zhu, and R. Zhang, "Novel permanent magnet motor drives for electric vehicles," *IEEE Trans. Ind. Electron.*, vol. 43, pp. 331–339, Apr. 1996.
[3] J. Y. Gan, K. T. Chau, Y. Wang, C. C. Chan, and J. Z. Jiang, "Design and analysis of a new permanent magnet brushless DC machine," *IEEE Trans. Magn.*, vol. 36, pp. 3353–3356, Sept. 2000.
[4] S. C. Park, B. H. Kwon, H. S. Yoon, S. H. Won, and Y. G. Kang, "Analysis of exterior-rotor BLDC motor considering the eddy current effect in the rotor steel shell," *IEEE Trans. Magn.*, vol. 35, pp. 1302–1305, May 1999.
[5] C. C. Chan, J. Z. Jiang, W. Xia, and K. T. Chau, "Novel wide range speed control of permanent magnet brushless motor drives," *IEEE Trans. Power Electron.*, vol. 10, pp. 539–546, Sept. 1995.